

EFFICIENT DESIGN OF AN 8-CONDUCTOR NONLINEAR KICKER FOR HEFEI ADVANCED LIGHT FACILITY USING A PYTHON-BASED TOOLCHAIN*

Weibo Hu¹, Xiao Ding¹, Wenbin Song^{†,1}, Lei Shang¹, Feng-lei Shang¹
¹University of Science and Technology of China, Hefei, China

Abstract

An 8-conductor nonlinear kicker (NLK) is proposed for the Hefei Advanced Light Facility (HALF) injection system. Its design is highly sensitive to conductor positions and must accommodate a vacuum chamber. This study develops an automated toolchain combining Opera-2D and Python with Bayesian optimization (Optuna) to search for feasible conductor configurations under strict magnetic and spatial constraints. A feasible design was obtained within 40 iterations, greatly improving R&D efficiency and offering a generalized approach for nonlinear magnet optimization in fourth-generation light sources.

INTRODUCTION

The Hefei Advanced Light Facility (HALF) is a fourth-generation diffraction-limited storage ring (DLSR) designed to achieve ultra-low emittance for providing high-brightness synchrotron radiation [1]. Such low emittance typically results in a narrow dynamic aperture, posing significant challenges to traditional off-axis injection schemes [2]. To achieve transparent top-up injection, a nonlinear kicker (NLK) is required to provide a specific magnetic field profile: a zero-field region at the center for the stored beam and a high-field region with a flat-topped peak for the injected beam.

The 8-conductor NLK is an ideal choice for HALF due to its structural simplicity and flexibility in field shaping. However, its design process faces two major obstacles. First, the field quality is extremely sensitive to the spatial coordinates of the conductors; sub-millimeter deviations can significantly shift the peak position, alter the magnetic flux density at the injection point, and degrade the central zero-field region. Second, a vacuum chamber with a substantial cross-section must be accommodated within the 8-conductor support structure to allow beam passage. This requires the NLK to not only produce the target field distribution but also ensure that the conductors are positioned sufficiently far from the origin to provide adequate clearance for the chamber [3, 4].

Traditionally, the design of such magnets relies on manual iterations using simulation software. This process is time-consuming and must be restarted from scratch whenever design specifications change, making targeted optimization

of magnetic performance difficult. To enhance design efficiency and reliability, this paper proposes an automated design framework. By integrating the Opera-2D simulation engine with a Python-based optimization environment, a toolchain capable of automating modeling, field extraction, and performance evaluation was developed. This approach enables rapid exploration of the design space and has successfully yielded feasible configuration schemes for the HALF NLK.

SYSTEM ARCHITECTURE AND MODELING

Design Objectives of the Nonlinear Kicker

The NLK for HALF employs a symmetric 8-conductor configuration to generate the required multipole magnetic field. The conductors are arranged around the axis of the stored beam, with their cross-sectional coordinates serving as the primary design variables. Due to the structural symmetry, the degrees of freedom are reduced to the position coordinates of two conductors in the first quadrant. Let Conductor A be the one closer to the origin and Conductor B be the other, with their coordinates denoted as (AX, AY) and (BX, BY) , respectively. The design objective is to create a field-free region at the center for the stored beam, while providing a deflection field for the injected beam at an injection point of $x = 7$ mm, with the magnetic field peak located near this position. Accordingly, several critical points are defined: the vertical magnetic field component (B_y) at $x = 0$ mm is denoted as By_0 , at $x = 1$ mm as By_1 , and at $x = 7$ mm as By_7 . The simulation was configured with a half-sine pulsed current featuring a pulse width of $1.6 \mu\text{s}$ and a peak of 3 kA. The design constraints require By_0 to be 0 Gauss, $By_1 \leq 25$ Gauss, and $By_7 \geq 800$ Gauss.

Automated Modeling based on Opera-2D and Python

To achieve automated modeling, a closed-loop workflow was implemented using the “operapy” interface, encompassing geometric parameter definition, mesh generation, time-varying current drive settings, finite element method (FEM) solving, and data extraction. This integration allows the solver to be invoked as a “black-box” function within the optimization loop, where the input is a set of coordinates and the output is the magnetic field data from the completed simulation.

* Work supported by the Fundamental Research Funds for the Central Universities (WK2310250134) and National Natural Science Foundation of China (No. 12205293)

† songwb@ustc.edu.cn

Spatial Constraints of the Vacuum Chamber

A critical constraint in the NLK design is the integration of the vacuum chamber. To ensure mechanical feasibility, an elliptical region centered at the origin is defined as a “forbidden zone”, as shown in Fig. 1. This forbidden zone is dimensioned to accommodate both the injected and stored beams while maintaining a safety margin from the conductors. During optimization iterations, any model that overlaps with this region or violates the minimum safety distance 1 mm is penalized and excluded from the search space. This ensures that the final design provides sufficient physical space for the vacuum chamber while maintaining high magnetic field quality, guaranteeing that the identified parameters are fully compatible with engineering requirements.

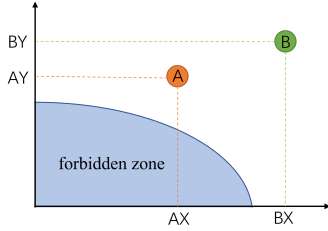


Figure 1: Schematic diagram of the NLK structure.

THE PYTHON-BASED DESIGN TOOLCHAIN

Workflow Integration

The automated toolchain is constructed as a closed-loop system. The process initiates with a set of conductor coordinates suggested by the optimizer (Optuna). These parameters are passed to a Python controller, which generates the simulation scripts for Opera-2D. Upon completion of the electromagnetic field computation by the solver, the Python script post-processes the results to extract the vertical magnetic field component (B_y) along the transverse axis. These values are then evaluated against the objective function, and the resulting feedback is sent back to the optimizer to guide the subsequent iteration. This seamless integration, as shown in Fig. 2, eliminates the need for manual data handling and significantly accelerates design iterations.

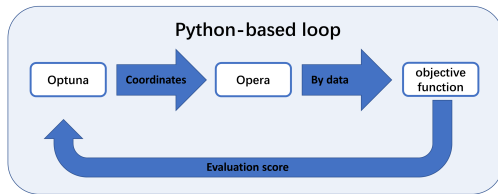


Figure 2: Workflow.

Bayesian Optimization Implementation via Optuna

Given the computational cost of electromagnetic simulations, Bayesian optimization was selected for its superior sample efficiency in high-dimensional spaces. In this

toolchain, the Tree-structured Parzen Estimator (TPE) sampler provided by the Optuna library is employed. Unlike random or exhaustive grid searches, this method constructs a probabilistic model of the objective function, concentrating the search in regions most likely to yield improvements. The optimization algorithm treats the 8-conductor coordinates as continuous variables, with their search ranges defined by the user based on empirical design knowledge.

Objective Function and Constraint Handling

The objective function is designed to quantitatively evaluate the performance of each model, encompassing both magnetic field distribution and conductor positioning, where a higher score indicates superior performance. It is derived from a comprehensive assessment of several metrics:

- Criterion 1: $By_7 \geq 800$ Gauss and the ratio $By_7/By_1 \geq 32$ (corresponding to 800/25).
- Criterion 2: The peak transverse coordinate (x_{peak}) must satisfy $6.5 \text{ mm} < x_{peak} < 7.5 \text{ mm}$.
- Criterion 3: No conductor must fall within the vacuum chamber’s “forbidden zone”.

Models satisfying all three criteria are considered “qualified”. Positive scores are assigned based on how closely x_{peak} approaches the target of 7.0 mm. Conversely, unqualified models are assigned negative scores based on the degree of deviation from the standards. The scores are normalized within a range of ± 1500 .

RESULTS AND DISCUSSION

Optimization Efficiency

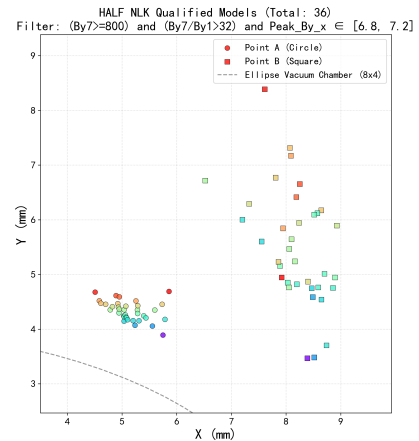


Figure 3: Distribution of qualified models.

The optimization process was conducted within a budget of 200 iterations. A total of 36 qualified AB pairs were found, with A and B corresponding one-to-one by color in Fig. 3. As shown in the convergence plot (Fig. 4), the objective function value, which integrates field quality and vacuum chamber constraints, improved rapidly within the first 80 trials. It is noted that the first qualified model appeared within the

first 20 simulations, while the first maximum-score model emerged within the first 40 iterations. The TPESampler effectively guided the search toward the feasibility region, identifying models that satisfy magnetic performance requirements while strictly avoiding the “forbidden zone” of the vacuum chamber. Compared to traditional manual tuning, which typically requires several days, the automated toolchain identified a feasible solution in only a few minutes.

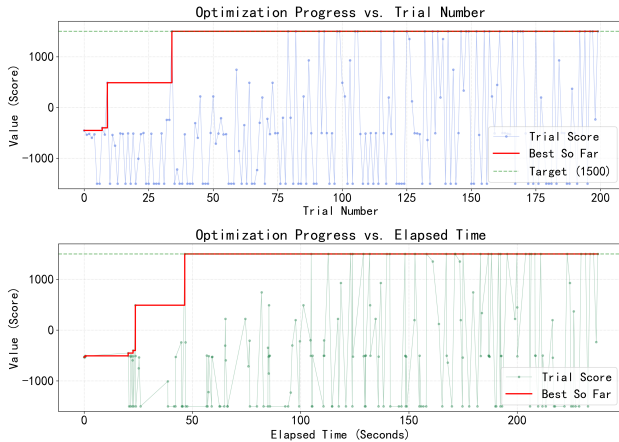


Figure 4: Evolution of scores over 200 iterations.

Final Design of the HALF NLK

The optimal conductor configuration for the HALF NLK was determined through the automated optimization design. The inner conductor A is positioned at (5.28 mm, 4.35 mm), and the outer conductor B at (8.16 mm, 5.24 mm). This design ensures a minimum clearance of 1 mm between the conductors and the vacuum chamber wall, as well as a minimum gap of 3 mm between Conductors A and B, thereby satisfying all mechanical and structural requirements. Figure 5 shows the B_y distribution of the model simulated in Opera-2D.

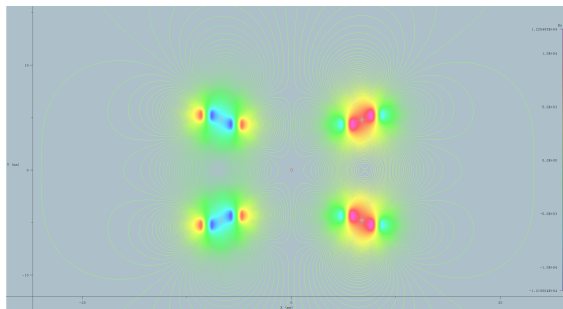


Figure 5: Magnetic field distribution of the model in Opera-2D.

Magnetic Performance Analysis

The magnetic field distribution of the optimized design is shown in Fig. 6. On the $y = 0$ plane, the vertical magnetic field component (B_y) within the central ± 1 mm, region is below 16.6 Gauss, effectively minimizing the perturbation to the stored beam. At the injection point ($x = 7$ mm), the

B_y component reaches 1591 Gauss, significantly exceeding the requirement of 800 Gauss. This provides a substantial margin for reducing the pulsed current intensity or for future upgrades and commissioning. Furthermore, the peak field position is situated in close proximity to the injection point. These results confirm that the automated design workflow can rapidly and reliably yield high-performance nonlinear magnet configurations that meet the stringent requirements of fourth-generation light sources.

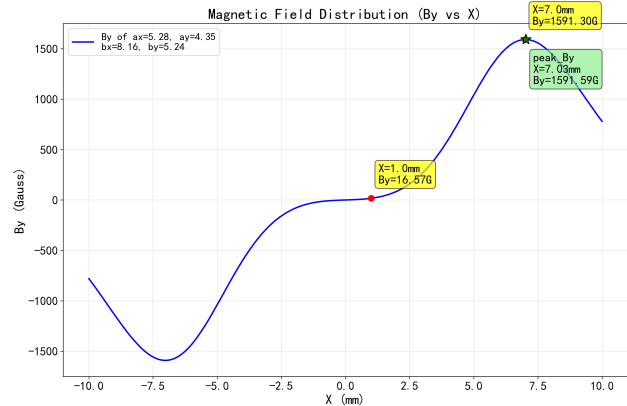


Figure 6: B_y data between $X \pm 10$ mm.

CONCLUSION

This paper presents an efficient Python-integrated design toolchain, which has been successfully applied to the design of the 8-conductor NLK for the HALF. By combining high-precision modeling in Opera-2D with the high sample efficiency of Bayesian optimization provided by Optuna, complex design challenges involving high-dimensional parameters and stringent spatial constraints were effectively addressed. Within a limited number of iterations, the optimization algorithm successfully identified a feasible configuration that satisfies both the magnetic field quality requirements for beam injection and the mechanical clearance constraints for the vacuum chamber. While manually tuned parameters can still yield several acceptable models through traditional trial-and-error debugging, the significance of this automated workflow lies not merely in replacing manual modeling attempts, but more importantly in providing a universal and reliable method for rapidly predicting the optimal model, thereby serving as a foundational tool for subsequent investigations into issues such as tolerance analysis and directional optimization. The actual 8-conductor NLK is not an infinitely long straight conductor model; rather, it has a finite length with unavoidable external wiring, which leads to end-field effects and degradation of the central zero-field region. Moreover, manufacturing tolerances in the physical realization are unavoidable and will likewise perturb the field profile. These issues will be quantitatively analyzed in subsequent studies, in which the automated workflow developed in this paper, with appropriate adaptations, will play an important role.

REFERENCES

- [1] Yi J and Zhenghe B, “Physics design and optimization of the fourth-generation synchrotron light sources”, *High Power Laser Part. Beams*, vol. 34, no. 10, pp. 104004-1–104004-10, 2022.
doi:10.11884/HPLPB202234.220136
- [2] P. Wang, P. Yang, G. Liu, Z. Bai, and W. Li, “Design and simulation of beam injection scheme for diffraction limited storage ring”, *High Power Laser Part. Beams*, vol. 35, no. 12, pp. 124006-1–124006-8, 2023.
doi:10.11884/HPLPB202335.230070
- [3] R. Ollier *et al.*, “Toward transparent injection with a multipole injection kicker in a storage ring”, *Phys. Rev. Accel. Beams*, vol. 26, no. 2, Feb. 2023.
doi:10.1103/physrevaccelbeams.26.020101
- [4] P. Alexandre *et al.*, “Transparent top-up injection into a fourth-generation storage ring”, *Nucl. Instrum. Methods Phys. Res. A*, vol. 986, p. 164739, 2021.
doi:10.1016/j.nima.2020.164739